Iterative APP interference cancellation for LDPC coded UWB communication

NSF EASI 2003 Report

Noah Jacobsen
ECE Department
University of California
Santa Barbara, 93106
{jacobsen@ece.ucsb.edu}

February 15, 2004

1 Introduction

Ultra wideband (UWB) communication is an emerging technology for high data rate, low power communication over short distances, e.g. wireless personal area networks. The IEEE 802.15.3a High Rate Task Group is currently standardizing UWB according to FCC approved power emissions in the 3.1 to 10.6 GHz frequency band. Evidently [1], multiband orthogonal frequency division multiplexing (OFDM) techniques are being favored to the original impulse radio approach. Inherent to either approach is a channel delay spread that spans a large number of data symbols. Given the large number of resolvable multipaths typical of a UWB channel, as illustrated in Figure 1, traditional equalization techniques are likely to be computationally infeasible. Thus, a major bottleneck for UWB transceiver design is the significant distortion caused by inter-symbol interference (ISI). Motivated by successful coding and modulation strategies [2], we propose a multiband UWB system equipped with powerful error correction coding and iterative receiver processing to combat UWB ISI. We find that the ISI is well approximated as Gaussian, thereby admitting the use of well known channel codes optimized for the classical AWGN channel. We have discovered the existence of an SNR threshold τ^*, analogous to the "waterfall region" of turbo-codes. At SNR, τ, greater than τ^*, arbitrarily accurate ISI estimation and subtraction is achievable. Conversely, if $\tau < \tau^*$, the bit error rate is strictly bounded away from zero.

Section 2 reviews relevant channel coding concepts, motivating the proposed UWB transceiver described in Section 4. Section 3 deals with the Gaussian approximation for UWB ISI, and simulation results are given in Section 5.

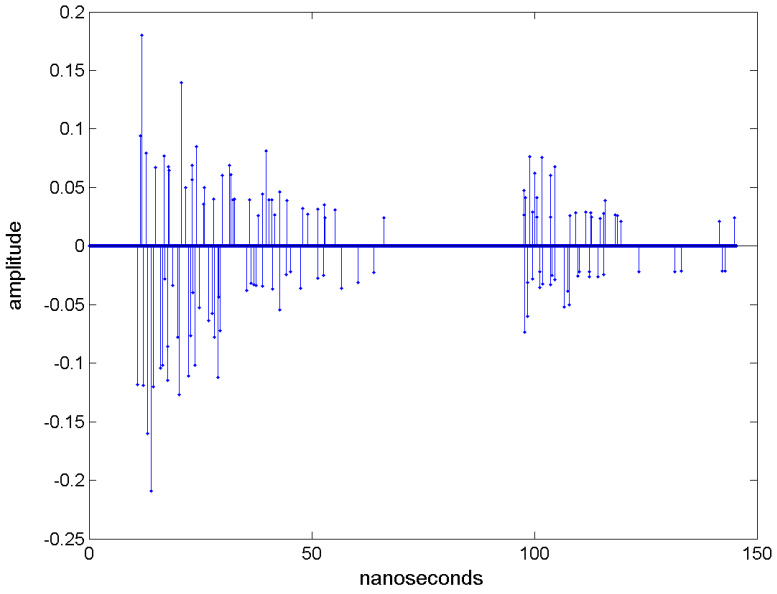

Figure 1: Typical UWB channel realization

2 Codes on graphs

Irregular low-density parity-check (LDPC) codes are known to approach the Shannon capacity [3] for a broad class of memoryless channels (see e.g. [4]). Gallager first introduced LDPC codes in his 1961 thesis [5]. Since then much attention has been given to this class of codes and the graphical framework for their representation and decoding [6, 7]. Any linear block code is equivalent to a bipartite graph of variable nodes, representing code symbols, and check nodes, representing parity check equations, as in Figure 2. If the *degree* of a node is the number of nodes it's connected to (alternatively the cardinality of its neighborhood), a *regular* (d_v, d_c) LDPC code has degree d_v variable nodes and degree d_c check nodes. Belief propagation decoding [8] on the graph of the dual of a linear block code is known to accurately approximate maximum a posteriori (MAP) probability decoding, and they are the same in the case of a cycle-free graph.

A powerful theory for the convergence of LDPC codes under belief propagation decoding and the "density evolution" algorithm for code threshold, τ^*, determination were developed in [9]. Ensembles of codes, distinguished by their underlying graphical structure, have been analyzed for many common memoryless channels. A particular instance of an LDPC code is obtained by sampling an element from its ensemble, the behavior of which is known to converge to its expected value as codeword length tends to infinity [10]. A memoryless channel is well-ordered by its degradation parameter, τ, if $\tau_1 > \tau_2$ implies that instance

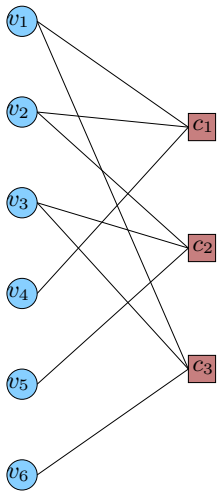

Figure 2: Tanner graph of a linear block code

1 distorts less than instance 2. If τ is greater than the threshold computed via density evolution, it's proven that the information bit error rate (BER) converges to zero in the length of the codeword and number of decoding iterations. Conversely, if $\tau < \tau^*$ then the BER is bounded away from zero. Thus, by comparing the threshold, also referred to as capacity, of ensembles of LDPC codes, one can compare their effectiveness on a given channel.

Optimal code construction requires the introduction of a more general class of irregular LDPC codes. To that end, define a *degree distribution* $\lambda(x) = \sum_{i \in \mathcal{I}} \lambda_i x^{i-1}$, over the set $\mathcal{I}$ of active degrees, to be the fraction λ_i of edges connected to a degree i node. Moreover, an *irregular* (λ, ρ) LDPC code has variable and check degrees distributed according to $\lambda(x)$ and $\rho(x)$ respectively. By allowing check and variable degrees to vary in this fashion, density evolution and its approximations have been used to find the best known codes for many common memoryless (e.g. erasures and AWGN) channels [10, 11].

Density evolution works by iteratively tracking arbitrary message densities, a computation made tractable with Fourier representations. In general, the algorithm is quite complicated and a number of approximations have been studied. The main result is that, on an AWGN channel, the messages themselves, in the form of log-likelihood ratios (LLRs), have a Gaussian density. In [12], a symmetry condition for density evolution is exploited to parameterize the message densities with only their mean. Equivalently, [13] proposes that the SNR of Gaussian messages be used to predict code convergence.

Perhaps the most intuitive technique for tracking convergence of iterative decoding is the extrinsic information transfer (EXIT) chart [14]. Here, the average mutual information between messages passed on the graph (the term extrinsic information coming from turbo-coding literature) and the information bits they are estimating is tracked throughout decoding. The mutual informa-

tion of decoder output is expressed as a function of input mutual information. This technique lends well to a graphical representation, immediately suggesting desirable constituent code properties. In the case of a Gaussian approximation for the message densities, the method is equivalent to [12], and has been used for irregular code optimization in a broader context [15, 16]. Further, EXIT charts have some interesting properties [17], due in part to the information theoretic quantity they describe.

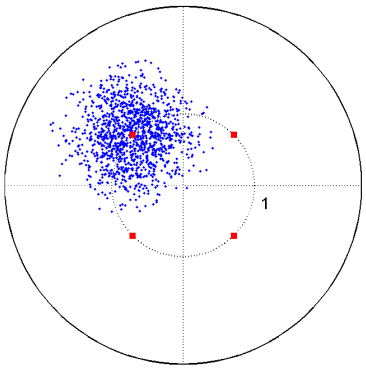

Figure 3: Noiseless QPSK reception

3 Gaussian approximation for UWB ISI

We first describe the discrete multipath impulse response typical of an indoor UWB channel. Let L denote the number of dominant reflecting bodies, and P_l the number of resolvable multipaths arriving from the l^{th} reflector, $l \in \{1, 2, 3, ..., L\}$. The effective (including pulse shape) complex baseband channel impulse response h is given by

$$h(n) = \sum_{l=1}^{L} \sum_{p=1}^{P_l} \alpha(l,p)\delta_{n,k(l,p)},$$

where $\delta_{n,k}$ is the Kronecker delta function and $k(l,p)$ is the delay associated with the p^{th} multipath component of the l^{th} reflector. The channel tap coefficients $\{\alpha(l,p)\}_{p=1}^{P_l}$ of the l^{th} reflector are typically modeled as correlated, exponentially decaying random variables, independent of the tap coefficients arising from any other reflector $l' \neq l$. The channel is normalized to have unit energy, i.e. $\|h\|^2 = 1$.

We employ a QPSK modulation, in which the transmitted symbol $s(t)$ in the t^{th} symbol interval is chosen randomly from $\{\exp(j\pi m/4) : m = 1, 3, 5, 7\}$. The tap-spaced transmitted signal is (1), where c is the characteristic function of $\{0, 1, 2, ..., T-1\}$, and T is the number of taps per symbol period. With w as

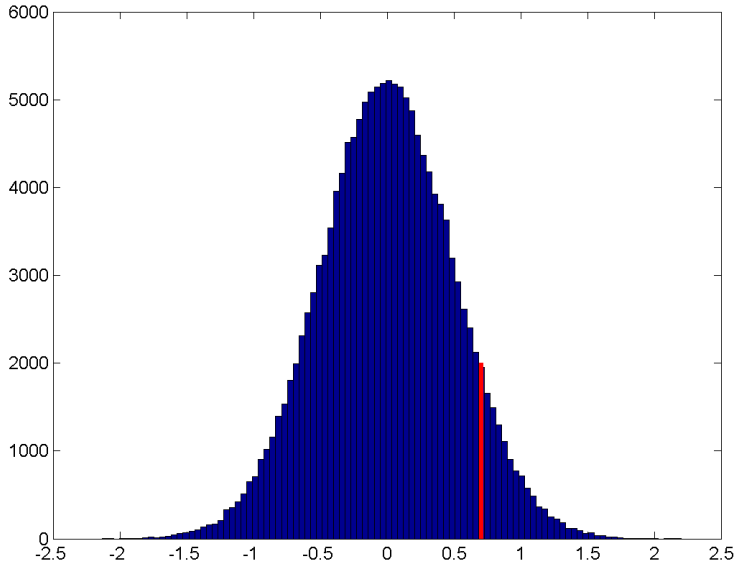

Figure 4: Measured ISI

zero-mean, variance σ^2 per dimension, complex Gaussian noise, the baseband received signal is (2).

$$\tilde{s}(n) = \sum_t s(t)c(n - tT) \tag{1}$$

$$y(n) = h(n) \star \tilde{s}(n) + w(n) \tag{2}$$

Consider a receiver whose front end, $h_{mf}(n) = h^*(-n)$, is matched to the effective channel impulse response. The output, sampled at the symbol rate, is given by

$$\begin{aligned} z(t) =& h_{mf}(n) \star y(n)|_{n=tT} \\ =& s(t) + isi(t) + \tilde{w}(t) \end{aligned} \tag{3}$$

where $\tilde{w}$ is again AWGN and isi is the ISI.

The ISI term is a summation that includes tap coefficients from every dominant reflector. Thus, for large values of L, typical of indoor radio channels, the central limit theorem dictates that the ISI density tends to the Gaussian. Figure 3 demonstrates the severity of UWB ISI, $z - \tilde{w}$, for the $s = \exp(j\pi 3/4)$ symbol. Furthermore, we have plotted a histogram of the real and imaginary components of the ISI in Figure 4. The density is evidently Gaussian. The noted x-intercept indicates the decision boundary of an adjacent symbol.

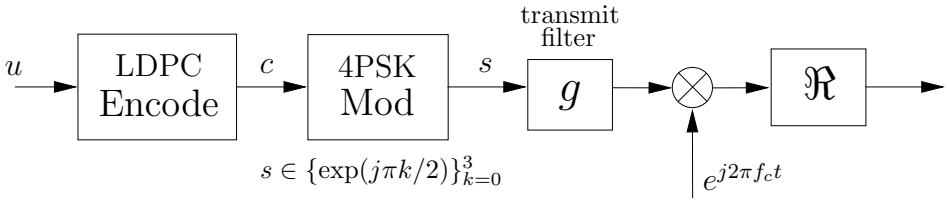

Figure 5: Transmitter

4 Coding for a UWB channel

The transmitter is a serial concatenation of irregular LDPC channel code and modulator, as in Figure 5. The transmit filter g is a 3 nsec rectified cosine. The -10 dB bandwidth is 650 MHz, thus constituting a UWB transmission by FCC 500 MHz minimum bandwidth and exemplifying a pulse shape for multiband UWB communication. By means of the Gaussian approximation for ISI, and assuming that decoding directly follows receive filtering, AWGN coding is optimal. Accordingly, a length 10^4, rate-1/2 irregular LDPC code optimized for the AWGN channel was constructed from [11].

We propose the iterative, soft interference estimating and subtracting UWB receiver of Figure 6. First, the receiver decodes based on the initial statistics z. Then, using probabilistic estimates of the transmitted symbol sequence, an estimated received sequence, and thus estimated ISI sequence $\hat{isi}$ is constructed. The updated statistics $z - \hat{isi}$ are formed, and decoding is performed again. Thus, iterative ISI estimation and subtraction is performed until the satisfaction of a stopping criterion. The receiver assumes knowledge of the variance of $isi + \tilde{w} - \hat{isi}$, and that this quantity remains Gaussian (which is reasonable by an inductive appeal to the central limit theorem). Given the independence of in-phase and quadrature components of complex Gaussian noise, the bit statistics are computed via the appropriate distances from $z - \hat{isi}$ to the real and imaginary axes.

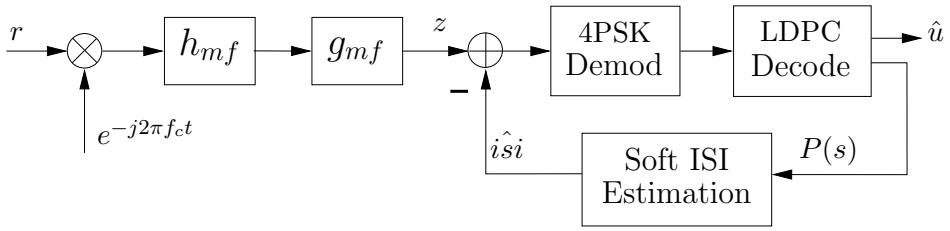

Figure 6: Receiver

5 Results

The proposed UWB transceiver was simulated on the IEEE 802.15.3a extreme ISI, non line-of-site (NLOS) channel model (#4). Figure 7 plots the information bit error rate per iteration. We note the existence of an SNR threshold at 3.5 dB, beyond which arbitrarily accurate ISI estimation and subtraction is achievable with a sufficient number of iterations. Thus, the power of the irregular LDPC channel code and effectiveness of the Gaussian approximation is demonstrated. The block error rate at the end of 5 iterations is reported in Figure 8. We see from this figure that, as SNR increases, the UWB receiver performance approaches that of an ISI free benchmark (AWGN) channel.

6 Conclusion

We have demonstrated the validity of a complex Gaussian approximation for ISI characteristic of an extreme multipath UWB channel with matched filter receiver. Soft interference estimation and subtraction is used to iteratively compensate for, or equalize, the effects of ISI. We have discovered the existence of an SNR threshold beyond which perfect ISI estimation is possible given enough receiver iterations. Future work includes a refinement of the above techniques, including more sophisticated channel modeling with appropriate adjustments to the coding scheme, and information theoretic comparisons.

7 Acknowledgements

I would like to thank Prof. Ryuji Kohno at Yokohama National University for his kind hospitality and meaningful discussions regarding UWB standardization and Japan's role therein. I'm also deeply indebted to my advisor, Prof. Upamanyu Madhow, at UCSB for inspiring comments and continuing guidance. Finally, I am grateful to the NSF and JSPS for generous financial and logistical support throughout the summer.

References

[1] "`http://www.ieee802.org/15/pub/TG3a.html`," IEEE 802.15 WPAN High Rate Alternative PHY Task Group 3a.

[2] N. Jacobsen and U. Madhow, "Reduced-complexity noncoherent communication with differential QAM and iterative receiver processing," *Proceedings of the 2003 Conference on Information Sciences and Systems*, Mar 2003.

[3] C.E. Shannon, "A mathematical theory of communication," *Bell Systems Technical Journal*, vol. 27, pp. 379–423, 623–656, 1948.

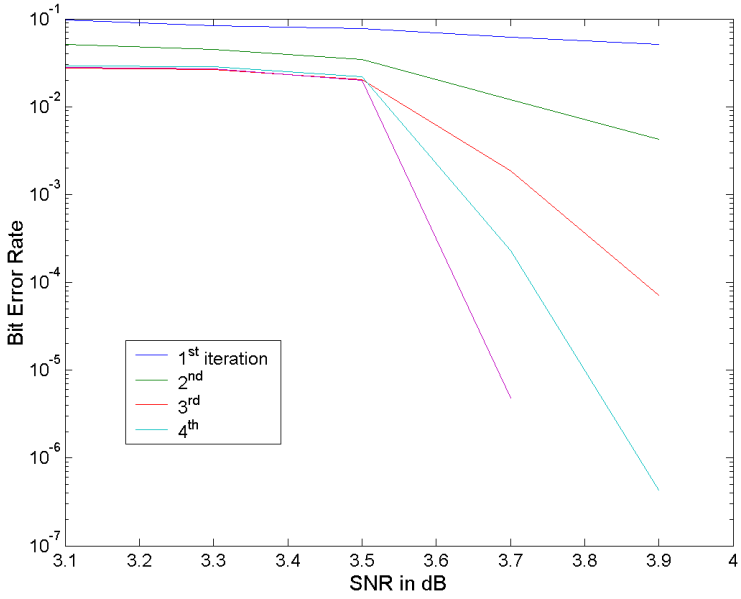

Figure 7: Bit error rate per iteration

[4] S.-Y. Chung, G.D. Forney, T.J. Richardson, and R. Urbanke, "On the design of low-density parity-check codes within 0.0045 dB of the Shannon limit," *IEEE Communications Letters*, vol. 5, no. 2, pp. 58–60, Feb. 2001.

[5] R. Gallager, "Low density parity check codes," *IRE Trans. Information Theory*, vol. 8, pp. 21–28, Jan. 1962.

[6] N. Wiberg, H.-A. Loeliger, and R. Kotter, "Codes and iterative decoding on general graphs," *European Trans. Telecommunications*, vol. 6, pp. 513–526, Sept. 1995.

[7] F.R. Kschischang, B.J. Frey, and H. Loeliger, "Factor graphs and the sum-product algorithm," *IEEE Trans. Information Theory*, vol. 47, no. 2, pp. 498–519, Feb. 2001.

[8] J. Pearl, *Probabilistic Reasoning in Intelligent Systems: Networks of Plausible Inference*, Morgan Kaufmann Publishers, San Mateo, CA, 1988.

[9] T.J. Richardson and R.L. Urbanke, "The capacity of low-density parity-check codes under message-passing decoding," *IEEE Trans. Information Theory*, vol. 47, no. 2, pp. 599–618, Feb. 2001.

[10] M.G. Luby, M. Mitzenmacher, M.A. Shokrollahi, and D.A. Spielman, "Improved low-density parity-check codes using irregular graphs," *IEEE Trans. Information Theory*, vol. 47, no. 2, pp. 585–598, Feb. 2001.

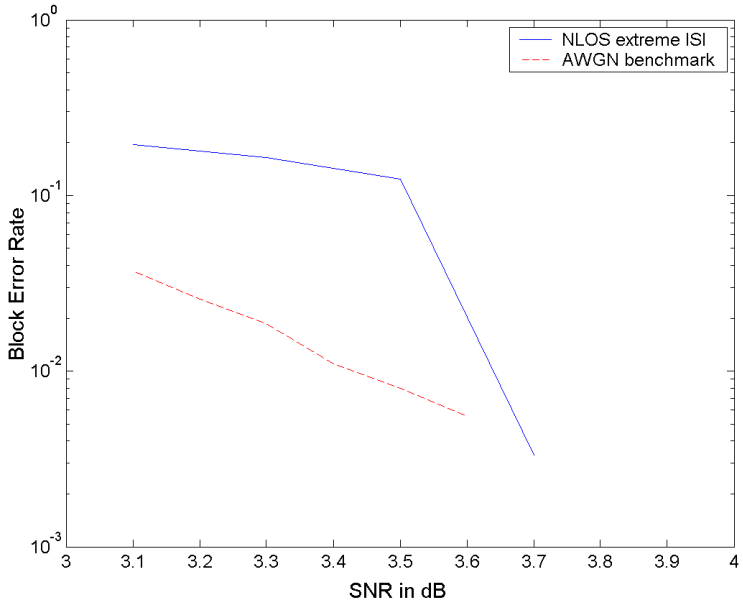

Figure 8: Block error rate

[11] T.J. Richardson, M.A. Shokrollahi, and R.L. Urbanke, "Design of capacity-approaching irregular low-density parity-check codes," *IEEE Trans. Information Theory*, vol. 47, no. 2, pp. 619–637, Feb. 2001.

[12] S.-Y. Chung, T.J. Richardson, and R.L. Urbanke, "Analysis of sum-product decoding of low-density parity-check codes using a Gaussian approximation," *IEEE Trans. Information Theory*, vol. 47, no. 2, pp. 657–670, Feb. 2001.

[13] H. El Gamal and A.R. Hammons Jr., "Analyzing the turbo decoder using the gaussian approximation," *IEEE Trans. Information Theory*, vol. 47, no. 2, pp. 671–686, Feb. 2001.

[14] S. ten Brink, "Convergence behavior of iteratively decoded parallel concatenated codes," *IEEE Trans. Communications*, vol. 49, no. 10, pp. 1727–1737, Oct. 2001.

[15] S. ten Brink, G. Kramer, and A. Ashikhmin, "Design of low-density parity-check codes for modulation and detection," *IEEE Trans. Communications*, submitted, 2003.

[16] M. Tüchler and J. Hagenauer, "EXIT charts of irregular codes," in *Proc. Conf. on Information Sciences and Systems (CISS)*, Princeton, NJ, USA, Mar. 2002.

[17] A. Ashikhmin, G. Kramer, and S. ten Brink, "Extrinsic information transfer functions: a model and two properties," in *Proc. Conf. on Information Sciences and Systems (CISS)*, Princeton, NJ, USA, Mar. 2002.